# Determination and analysis of basic physical and contact mechanics parameters of quinoa seeds by DEM

Linrong Shi[1], Wuyun Zhao[1*], Bugong Sun[1], Wei Sun[1], Gang Zhou[2]
(1. *College of Mechanical and Electrical Engineering, Gansu Agricultural University, Lanzhou 730070, China*;
2. *Institute of Dryland Agriculture, Gansu Academy of Agricultural Sciences, Lanzhou 730070, China*)

**Abstract:** Quinoa is an ancient crop that is nutritious, balanced, and suitable for most people. However, it has not been known and sought by the public until modern times. In recent years, quinoa has been intensively known and widely grown in China. Quinoa mechanized production machines have also been developed. With the help of DEM, we design and optimize the quinoa combined seeder, improving seeding efficiency and quality. In this paper, the basic physical and contact mechanics parameters required for the Hertz-Mindlin (no slip) of quinoa seeds in EDEM software were determined. The coefficient of rolling friction of quinoa seeds was calibrated on DEM, and which of Long Quinoa 4 is 0.043, and that of Meng Quinoa 4 was 0.016. Meanwhile, we can find that the coefficient of rolling friction strengthens the shape to restrict rolling and weakens the shape to increase rolling. The above research provides simulation parameters for the design and optimization of quinoa seed seeding machinery.

**Keywords:** quinoa seeds, physical parameters, contact parameters, calibration, DEM
**DOI:** 10.25165/j.ijabe.20231605.7837

**Citation:** Shi L R, Zhao W Y, Sun B G, Sun W, Zhou G. Determination and analysis of basic physical and contact mechanics parameters of quinoa seeds by DEM. Int J Agric & Biol Eng, 2023; 16(5): 35–43.

## 1 Introduction

Computer simulation has the advantages of short cycle time, economic costs, and independence from farming. It has been widely used in farm machinery research for development in recent years[1]. Of these, Discrete Element Method (DEM) techniques are used for analyzing complex dynamic discontinuous mechanical discrete systems, which have demonstrated advantages in the study of agricultural materials[2], including maize[3], rice[4], wheat[5], potato[6], flax[7], cereals and canola[8], and have been applied to practically most of the crops. In DEM, the agricultural material model can be established by spherical particle or spherical aggregation method. DEM simulation can observe seeds trajectory, motion, and collision behavior and the resistance and motion process of farm machinery and its components. This is based on the interaction mechanism between agricultural materials and implements that can be deeply explored to guide the design and optimization of farm machinery[9]. Accurate and reliable parameters are the basis for efficient simulation results. For agricultural production, interactions with seeds occur at every step of the process, from seeding to processing. The movement behavior of seeds is influenced by their physical and mechanical properties, especially among seeds[8]. The parameters required for DEM can be divided into two categories. Material properties and contact mechanical properties[9]. Material properties include shape, size distribution, density, elastic and shear modulus, Poisson's ratio, and yield strength. The critical interaction properties are restoring forces, static and rolling friction, plastic or viscous damping, and adhesion[10]. There are two ways to obtain simulation parameters[2], by the experimental procedure the first method gets parameters that are easy to measure, and the second method is obtained by simulation calibration for parameters that are more difficult to measure directly[11].

The quinoa called "Mother" of "Food" originated in Peru[12]. Quinoa contains twice as much protein as rice, minerals, vitamins, and lysine, which is missing in most grains. Quinoa is easy to cook and digest, has a unique taste, tones the body, prevents disease, soothes the three highs, and is suitable for all groups, making it is safe, healthy, nutritious, and natural food material[13]. China's annual demand for grain is staggering as a significant consumer of grain production. To improve quinoa production, mechanization is needed to provide data reference to facilitate the development of quinoa-related machinery, mainly on DEM to design and optimize the seeding and harvesting machine.

In this study, parameters were determined and calibrated for two quinoa varieties, Long Quinoa 4 and Meng Quinoa 4, grown in Gansu Province. Since quinoa's tiny seeds make it difficult to determine the coefficient of rolling friction, it be calibrated with the help of DEM.

## 2 Material and methods

The basic physical parameters of quinoa seeds include triaxial dimensions, thousand-grain weight, mass density, bulk density, and moisture content. In addition, the contact mechanics parameters consist of the coefficient of static and rolling friction among seeds and between seeds and other materials and the coefficient of restitution, all of which can be determined by an experiment.

**Received date:** 2022-06-13 **Accepted date:** 2023-05-10
**Biographies: Linrong Shi**, PhD, Associate Professor, research interest: key technologies and equipment for precision seeding in northwest cold and arid zone, Email: shilr@gsau.edu.cn; **Bugong Sun**, PhD, Professor, research interest: crop production equipment project in northern dry zone, Email: sunbg@gsau.edu.cn; **Wei Sun**, Professor, research interest: agricultural mechanization engineering, Email: sunw@gsau.edu.cn; **Gang Zhou**, Master, Research assistant, research interest: key technologies and equipment for precision seeding in northwest cold and arid zone, Email: 2987869252@qq.com.
***Corresponding author: Wuyun Zhao**, PhD, Professor, research interest: agricultural mechanization engineering. Mechanical and Electrical Engineering College, Gansu Agricultural University, Lanzhou 730070, China. Tel: +86-15101322368, Email: zhaowy@gsau.edu.cn.

### 2.1 Shape and volume distribution

The quinoa shape is pill-shaped, and the middle part is full and bulging, is approximately cylindrical. 500 quinoa seeds were randomly selected (Long Quinoa 4 (LQ) and Meng Quinoa 4 (MQ)). It can be measured by length ($L$), width ($W$), and thickness ($T$) with digital vernier calipers (accuracy: 0.02 mm)[8], as shown in Figure 1. The average length $L$ of Long Quinoa 4 seeds is 2.23 mm, and the average width $W$ is 2.17 mm, and the average thickness $T$ is 1.21 mm. The average length $L$ of MQ seeds is 2.00 mm, and the average width $W$ is 1.86 mm, and the average thickness $T$ is 1.08 mm. The volume distribution can be analyzed approximately and derived from the volume $V=LWT$. Their volume distribution pattern is shown in Figure 2.

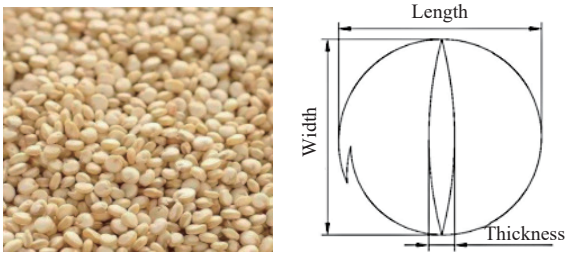


a. Shape b. 3 directional dimensions

Figure 1 Shape and 3 direction dimensions of quinoa seeds

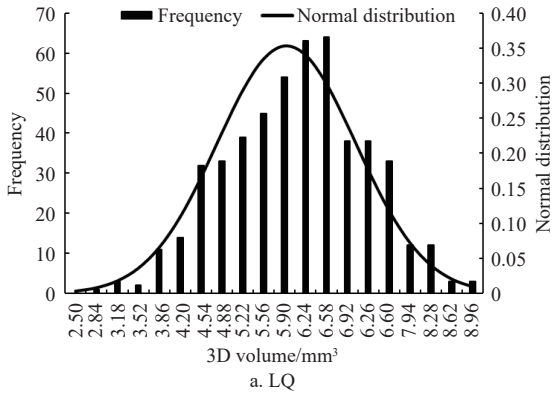


a. LQ

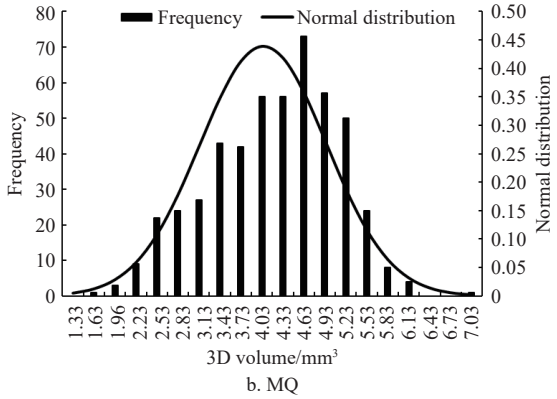


b. MQ

Figure 2 Volume distribution of quinoa seeds

From Figure 2, we can know that the volume distribution of quinoa seeds is normally distributed, and the standard deviation of LQ is 0.19, and that of MQ quinoa seeds is 0.22.

### 2.2 Thousand-grain weight

Thousand-grain weight is an essential index of seed quality[14]. LQ and MQ were randomly selected, each with 1000 seeds. The weight was measured using a BM-120 electronic balance (accuracy 0.01 g). The measurement results are listed in Table 1.

**Table 1 Thousand-grain weight of quinoa seeds (g)**

| Species | Group | | | | | Average |
|---|---|---|---|---|---|---|
| | 1 | 2 | 3 | 4 | 5 | |
| LQ | 3.90 | 3.92 | 3.67 | 3.76 | 3.84 | 3.818 |
| MQ | 3.10 | 2.99 | 3.03 | 2.97 | 3.05 | 3.028 |

### 2.3 Mass density

Mass density defines a quantity of how much material is contained in a unit volume of seed. LQ and MQ were randomly selected, each with 1000 seeds. The mass was first measured. Then the volume was measured by the drainage method using a 10 mL measuring cylinder. Measuring instruments are shown in Figure 3. The mass density was calculated by $\rho=m/V$. The results are listed in Table 2.

a. BM-120 electronic balance b. 10 mL measuring cylinder

Figure 3 Instruments for the determination of mass density

**Table 2 Mass density of quinoa seeds**

| Species | Parameter | Group | | | Average |
|---|---|---|---|---|---|
| | | 1 | 2 | 3 | |
| LQ | Mass $m$/g | 3.84 | 3.76 | 3.92 | |
| | Volume $V$/mL | 2.98 | 2.99 | 3.03 | |
| | Mass density $\rho_1$/(g·mL$^{-1}$) | 1.29 | 1.26 | 1.29 | 1.28 |
| MQ | Mass $m$/g | 3.08 | 3.03 | 3.04 | |
| | Volume $V$/mL | 2.28 | 2.25 | 2.23 | |
| | Mass density $\rho_2$/(g·mL$^{-1}$) | 1.35 | 1.35 | 1.36 | 1.35 |

From Table 2, it can be seen that the mass density of MQ is greater than that of LQ.

### 2.4 Bulk density

The bulk density calculation is like mass density. Seeds are taken in groups of 200, 400, 600, 800, and 1000, using a 10 mL measuring cylinder to measure the volume and the BM-120 electronic balance to the mass. The results are listed in Table 3.

**Table 3 Bulk density of quinoa seeds**

| Species | Parameter | Group | | | | | Average |
|---|---|---|---|---|---|---|---|
| | | 200 | 400 | 600 | 800 | 1000 | |
| LQ | Mass $m$/g | 0.74 | 1.58 | 2.32 | 3.02 | 3.81 | |
| | Volume $V$/mL | 0.61 | 1.26 | 1.83 | 2.38 | 2.99 | |
| | Bulk density $\rho_3$/(g·mL$^{-1}$) | 1.21 | 1.25 | 1.27 | 1.27 | 1.27 | 1.25 |
| MQ | Mass $m$/g | 0.60 | 1.24 | 1.75 | 2.46 | 3.03 | |
| | Volume $V$/mL | 0.48 | 0.95 | 1.34 | 1.84 | 2.24 | |
| | Bulk density $\rho_4$/(g·mL$^{-1}$) | 1.25 | 1.31 | 1.31 | 1.34 | 1.35 | 1.33 |

From Table 3, the bulk density of LQ is less than the mass density, and the same as MQ. Also, the bulk density of MQ is greater than that of LQ.

### 2.5 Moisture content

The moisture content strongly influences the mechanical

properties of the seeds in a similar way that thermoplastics or metals are influenced by the effect of temperature. Water modifies seeds' surface properties and bulk properties mainly by softening the seed structure and filling the internal stomata. Seed moisture content is a crucial physiological indicator of seeds that will affect seed germination and the design of operational equipment. LQ and MQ were randomly selected, each with 1000 seeds in 3 groups. The mass was measured using BM-120 electronic balance before drying, and then it was weighed after continuous drying at 105° during 24 h using the oven (as shown in Figure 4). The wet and dry bases moisture content was calculated by Equations (1) and (2), respectively, and the results are shown in Table 4.

**Table 4 Moisture content of quinoa seeds**

| Species | Parameters | Group | | | Average |
|---|---|---|---|---|---|
| | | 1 | 2 | 3 | |
| LQ | Mass before drying/g | 3.84 | 3.76 | 3.92 | |
| | Mass after drying/g | 3.34 | 3.26 | 3.41 | |
| | Water content/g | 0.50 | 0.50 | 0.51 | |
| | Wet basis moisture content/% | 13 | 13 | 13 | 13 |
| | Dry basis moisture content/% | 15 | 15 | 15 | 15 |
| MQ | Mass before drying/g | 3.08 | 3.11 | 3.04 | |
| | Mass after drying/g | 2.81 | 2.83 | 2.74 | |
| | Water content/g | 0.27 | 0.28 | 0.30 | |
| | Wet basis moisture content/% | 9 | 9 | 10 | 9 |
| | Dry basis moisture content/% | 10 | 10 | 11 | 10 |

$$M_s = \frac{G_w}{G_s} = \frac{G_s - G_g}{G_s} \times 100\% \quad (1)$$

$$M_g = \frac{G_w}{G_g} = \frac{G_s - G_g}{G_g} \times 100\% \quad (2)$$

where, $M_s$ is wet basis moisture content, %; $M_g$ is dry basis moisture content, %; $G_w$ is mass of water in seeds, g; $G_s$ is mass of seeds before drying, g; $G_g$ is mass of seeds after drying, g.

a. ovens b. weighing of quinoa seeds

Figure 4 Instrument for determining the moisture content

### 2.6 Poisson's ratio

Poisson's ratio is the transverse strain to longitudinal strain ratio when the material is under stress in the proportional limit [7]. Seed moisture content significantly influences Poisson's ratio size[5]. A mass spectrometer measured the deformation in the axial and radial directions after the compression experiment using a flat-topped cylinder[15]. The experiment was conducted using a probe to compress a seed placed on a pressure-bearing table at a rate of 1 mm/min until they ruptured. After the repeated experiments, quinoa seeds ruptured when the probe was loaded to 0.35-0.45 mm. The radial deformation before and after loading was measured using digital vernier calipers. The Poisson's ratio was calculated by Equation (3). The results are listed in Table 5.

$$\mu = \frac{W_f - W_a}{T_f - T_a} = \left| \frac{h_w}{h_t} \right| \quad (3)$$

where, $\mu$ is Poisson's ratio; $h_w$ is tradial deformation after compression, mm; $h_t$ is axial deformation after compression, mm; $W_f$ is width before compression, mm; $W_a$ is width after compression, mm; $T_f$ is thickness before compression, mm; $T_a$ is thickness after compression, mm.

**Table 5 Poisson's ratio of quinoa seeds**

| Species | Deformation | Number | | | | | | | | | | Average | Poisson's ratio |
|---|---|---|---|---|---|---|---|---|---|---|---|---|---|
| | | 1 | 2 | 3 | 4 | 5 | 6 | 7 | 8 | 9 | 10 | | |
| LQ | $h_w$ | 0.04 | 0.03 | 0.04 | 0.04 | 0.02 | 0.05 | 0.02 | 0.14 | 0.01 | 0.07 | 0.04 | 0.24±0.11 |
| | | 0.06 | 0.06 | 0.03 | 0.02 | 0.05 | 0.01 | 0.01 | 0.04 | 0.06 | 0.04 | | |
| | $h_t$ | 0.18 | 0.15 | 0.16 | 0.16 | 0.17 | 0.20 | 0.05 | 0.30 | 0.13 | 0.19 | 0.17 | |
| | | 0.17 | 0.25 | 0.16 | 0.17 | 0.17 | 0.12 | 0.14 | 0.18 | 0.21 | 0.12 | | |
| MQ | $h_w$ | 0.06 | 0.02 | 0.03 | 0.05 | 0.02 | 0.05 | 0.02 | 0.03 | 0.01 | 0.01 | 0.03 | 0.25±0.13 |
| | | 0.05 | 0.03 | 0.06 | 0.03 | 0.07 | 0.03 | 0.04 | 0.02 | 0.03 | 0.01 | | |
| | $h_t$ | 0.15 | 0.14 | 0.14 | 0.13 | 0.15 | 0.11 | 0.12 | 0.12 | 0.14 | 0.13 | 0.14 | |
| | | 0.15 | 0.20 | 0.13 | 0.11 | 0.13 | 0.15 | 0.13 | 0.15 | 0.14 | 0.14 | | |

### 2.7 Modulus of elasticity

The modulus of elasticity is the ratio of stress to deformation when an object is subjected along one direction in the elastic deformation. Non-sphere shape of quinoa seeds belongs to anisotropic materials. Assuming that the deformation is small during the measurement of the angle of repose, it can be assumed that quinoa seeds is isotropic. The complex stress distribution is formed while compressing. It is related to contact pressure, contact area and Poisson's ratio. Pressure is obtained by a mass spectrometer (TA-XT, China), as shown in Figure 5a. Two radii of curvature $R_1$ $R_2$ and deformation $D$ are recorded by camera. When the procedure was started, the probe was adjusted to be close to quinoa seeds on support table. Then the probe (5 mm diameter) compressed at a speed of 1 mm/min until compression depth was 0.5 mm. When the deformation is close to 1/10 of the deformation at the rupture point, the probe stops moving downward and moves upward slowly (unloading), records the pressure and the corresponding deformation data, and makes a hysteresis curve of the relationship between pressure and deformation, and calculates the modulus of elasticity from the hysteresis curve of the unloading and loading curves by Equation (5)[16]. A schematic diagram of quinoa compression is shown in Figure 5b. The elasticity and shear modulus was calculated from Equations (4) and (5), respectively. The results are listed in Table 6.

$$E = 1.502F(1+\mu^2)\left[\left(\frac{1}{R_1} + \frac{1}{R_2}\right)/D^3\right]^{\frac{1}{2}} \quad (4)$$

$$G = \frac{E}{2(1+\mu)} \quad (5)$$

where, $E$ is modulus of elasticity, MPa; $F$ is pressure on the quinoa seed, N; $D$ is deformation at the contact, mm; $\mu$ is Poisson's ratio; $R_1$ is minimum radius of curvature at the contact, mm; $R_2$ is maximum radius of curvature at the contact, mm.

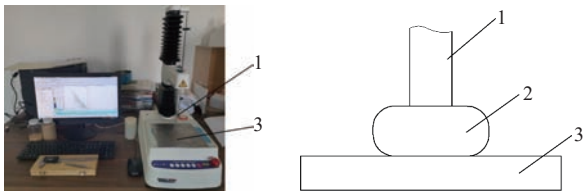


a. Mass spectrometer b. Schematic diagram

1. Probe; 2. Quinoa seeds; 3. Support table

Figure 5 Determination schematic diagram of modulus of elasticity and devices

**Table 6 Elasticity and shear modulus of quinoa seeds (MPa)**

| Species | Elasticity modulus | Shear modulus |
|---|---|---|
| LQ | 29.287±3.391 | 11.809 |
| MQ | 20.062±2.057 | 8.024 |

### 2.8 Coefficient of static friction

Friction force needs to be considered when designing seed production machinery. The affecting factor involve the material type, the contact surface's roughness, et al. The contact materials include steel plates, acrylic plates, and quinoa seeds (quinoa seeds were fixed to the acrylic plate), as shown in Figures 6a and 6b. The static friction angle of quinoa seeds was measured by the traditional slope method, and the principle of measurement and measuring instrument are shown in Figures 6c and 6d. When performing the experiment, first the contact plate is placed on the experiment bench, then a quinoa seed is placed above the contact plate about 150 mm from the fixed end, the other end of the plate is slowly raised until the seed start to fall and stop. The friction angle is measured with a digital protractor. The coefficient of static friction was obtained with $\mu_1=\tan\theta$ [17]. The results are listed in Table 7.

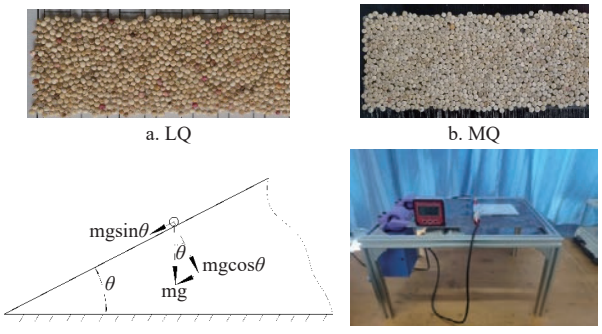


a. LQ b. MQ

c . Principle of measurement d. Instruments by slope method

Figure 6 Experimental materials and instruments

**Table 7 The measuring results of coefficient of static friction**

| Species | Steel | | Acrylic | | Quinoa seeds | |
|---|---|---|---|---|---|---|
| | $\theta$/° | $\mu_1$ | $\theta$/° | $\mu_1$ | $\theta$/° | $\mu_1$ |
| LQ | 20.48 | 0.376 | 20.67 | 0.381 | 14.99 | 0.269 |
| MQ | 20.68 | 0.381 | 21.07 | 0.388 | 15.27 | 0.274 |

### 2.9 Coefficient of restitution

The coefficient of restitution affects the ability of an object to recover from collision deformation. Since it is a form of seed potential energy conversion into kinetic energy during the energy conversion process, its influence on the seed flow process is negligible. It is measured by the free-fall method, and the principle of measurement as shown in Figure 7a. The collision material includes steel plate, acrylic plate, and quinoa seeds plate. The quinoa seeds are more affected by air resistance as are lighter and smaller, thus the drop height is set at 100 mm. When performing the experiment, firstly, the quinoa seed was placed 100 mm above the collision material plate, then the seed process was recorded by smartphone when seeds started to fall, with a steel ruler in the background, as shown in Figure 7b. The coefficient of restitution is calculated by Equation (8). The results are shown in Table 8.

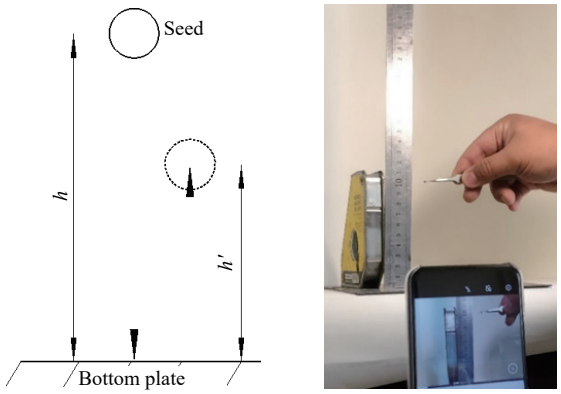


a. Principle of measurement b. Measurement field

Figure 7 Principle measurement of the coefficient of restitution and Field

**Table 8 The measuring results of coefficient of restitution**

| Material | LQ | | | MQ | | |
|---|---|---|---|---|---|---|
| | $h$/ mm | $h$/ mm | $e$ | $h$/ mm | $h$/ mm | $e$ |
| Steel | 17.3 | 100 | 0.4560 | 24.4 | 100 | 0.517 |
| Acrylic | 22.5 | 100 | 0.3936 | 27.8 | 100 | 0.470 |
| Quinoa seeds | 12.3 | 100 | 0.3250 | 16.2 | 100 | 0.377 |

$$e = \left|\frac{v_2' - v_1'}{v_2 - v_1}\right| = \left|\frac{v_2'}{v_2}\right| = \sqrt{\frac{h'}{h}} \quad (6)$$

where, $v_2 = -\sqrt{2gh}$, $v_2' = -\sqrt{2gh'}$, and $e$ is coefficient of restitution; $g$ is acceleration of gravity, m/s$^2$; $h$ is dropping height, mm; $h'$ is bounce height, mm; $v_1$ is velocity of plate before collision, m/s, initially $v_1$ is 0; $v_2$ is velocity of seed before collision, m/s; $v_1'$ is velocity of plate after collision, m/s; $v_1'$ is 0; $v_2'$ is velocity of seed after collision, m/s.

### 2.10 Repose angle

Experiments were conducted with round aluminum tubes (inner wall diameter 30 mm, height 200 mm) and round acrylic tubes (inner wall diameter 60 mm and height 200 mm) for forming the repose angle of quinoa seeds. During the experiment, the axis of the round tube was placed vertically on the horizontal surface. Quinoa seeds (70 g in round acrylic tube and 20 g in a round aluminum tube) were injected into the tube, as shown in Figure 8a. The round acrylic tube was lifted at a speed of 50 mm/s, then the seeds naturally fell and piled up under the gravity to form a cone shape, the bottom angle of which was the repose angle. To obtain more stable values, four repose angles along the $x$ and $y$ axes direction were measured, and the coordinate system is created with the positive direction of the $x$-axis horizontally to the right and the positive direction of the $y$-axis numerically downwards, as shown in Figures 8b-8d. Side pictures were taken by camera and imported

into CAXA electronic drawing board software (Beijing Digital Grand Technology Company. China) to mark the repose angle, this is $\theta_1$ and $\theta_2$ along the $x$-axis, $\theta_3$ and $\theta_4$ along the $y$-axis direction, respectively. Five trials were conducted and averaged. The results are listed in Table 9.

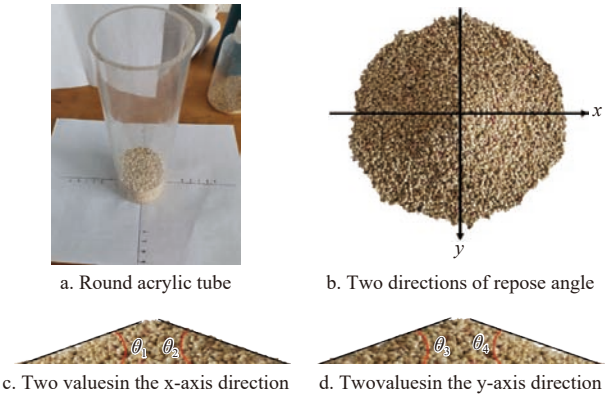


a. Round acrylic tube b. Two directions of repose angle

c. Two valuesin the x-axis direction d. Twovaluesin the y-axis direction

Figure 8 Measurement of repose angle of quinoa seeds

**Table 9 Repose angle of quinoa seeds (°)**

| Species | Aluminum tube | | | Acrylic tube | | |
|---|---|---|---|---|---|---|
| | $x$ | $y$ | Average | $x$ | $y$ | Average |
| LQ | 18.35 | 19.21 | 18.78 | 26.53 | 27.33 | 26.93 |
| MQ | 18.93 | 18.69 | 18.82 | 27.77 | 27.59 | 27.68 |

From Table 9, it can be seen that the repose angles formed in two containers differed significantly. Repose angle is related to the container material and size, and seed number. As the difference in friction between the two containers and the quinoa seeds was small, then it suggests that the number of seeds also influences the repose angle.

## 3 Results and analysis

Since quinoa seeds are tiny, the experimental method makes it difficult to determine their coefficient of rolling friction. This paper calibrates the coefficient of rolling friction on DEM to simulate the repose angle to approximate the actual repose angle. The simulation calibration model needs to be established before the parameter calibration.

### 3.1 Simulation modeling

The seed shape is an essential input in simulation, and the accuracy affects the prediction results. Quinoa seeds are flat and spherical, which belong to non-spherical seeds. Irregularly shaped seeds affect the energy conversion process, precisely the efficiency of converting the gravitational potential energy into the kinetic energy of rotation. Complex shape seeds are usually built using the sphere aggregation method. This method has been successfully applied to model a variety of crops[18,19]. Since the seed contact is done through sub-sphere contact, the number of sub-spheres reduce simulation efficiency[18]. Although an increase in the number can provide model smoothness[20], more sub-spheres filling the model increase computational time[21]. Barrios et al.[10] compared the repose angle under rotating drum experiment of iron ore models built with single spheres and the sphere aggregation method. They found better agreement between the experiment and simulation model by the sphere aggregation method with rolling friction coefficient. The rice seed model produced by the spherical aggregation method with the coefficient of rolling friction accurately simulated the repose angle and the hopper discharge time[11]. The coefficient of rolling friction between seeds and boundary has a negligible effect on the repose angle. Based on the above considerations, to improve simulation efficiency and accuracy of simulation, a small number of sub-spheres were used to fill the quinoa model and calibrate the coefficient of rolling friction between models.

The quinoa models were established with 4 sphere particles. Firstly, 3D model was established with SolidWorks 2018 software (Dassault Systems SOLIDWORKS Corp, USA), then the model was imported into EDEM 2018 software and filled with the sphere aggregation method[4], as shown in Figure 9. The simulation model for forming repose angle was established and the simulation experiments were conducted. The formation process of repose angle is shown in Figure 10. The contact model Hertz-Mindlin (no slip) between seeds, seeds and other material are the selected. The seeds volume distribution obeys normal distribution, and the standard deviation of LQ quinoa seeds is 0.19, and that of MQ seed distribution is 0.22. The time step is 30% rayleigh time step. The grid size is 2.49 mm for LQ and 2.00 mm for MQ. Simulation parameters are listed in Table 10.

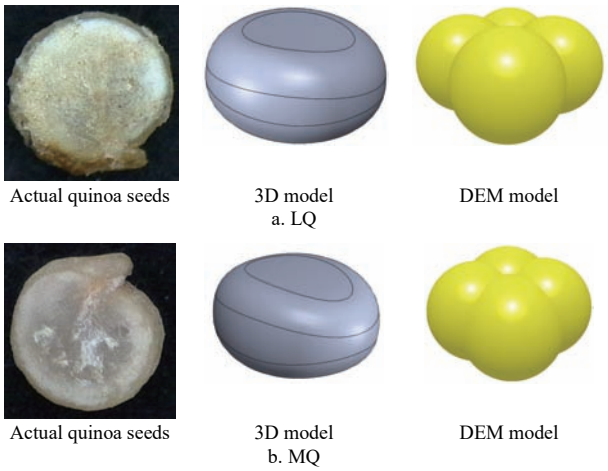

Actual quinoa seeds 3D model DEM model

a. LQ

Actual quinoa seeds 3D model DEM model

b. MQ

Figure 9 3D model and DEM of quinoa seeds

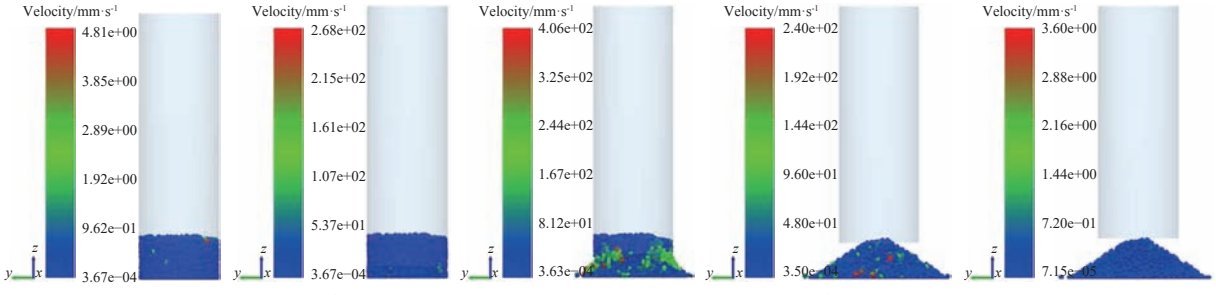


a. 0.1 s b. 0.3 s c. 0.6 s d. 0.8 s e. 0.12 s

Figure 10 Formation process of repose angle of quinoa seeds

**Table 10 Simulation parameters**

| Parameters | Value |
|---|---|
| Poisson's ratio of LQ/MQ | 0.24/0.25 |
| Density of LQ/MQ/(kg·m$^{-3}$) | 1280/1350 |
| Modulus of elasticity/×10$^7$ Pa | 2.91/2.01 |
| Shear modulus of LQ/MQ/×10$^7$ Pa | 1.18/0.80 |
| Coefficient of restitution of LQ/MQ | 0.325/0.377 |
| Coefficient of static friction between seeds of LQ/MQ | 0.269/0.274 |
| Poisson's ratio of acrylic /aluminum | 0.37/0.33 |
| Density of acrylic /aluminum /kg·m$^{-3}$ | 1180/7850 |
| Elasticity modulus of acrylic /aluminum /×10$^9$ Pa | 2.33/720 |
| Shear modulus of acrylic /aluminum /×10$^9$ Pa | 8.50/271 |
| Coefficient of restitution between LQ/MQ and acrylic | 0.393/0.47 |
| Coefficient of restitution between LQ/MQ and aluminum | 0.456/0.517 |
| Coefficient of static friction between LQ/MQ and acrylic | 0.381/0.388 |
| Coefficient of static friction between LQ/MQ and aluminum | 0.376/0.381 |
| Coefficient of rolling friction between LQ/MQ and acrylic | 0.093/0.093 |
| Coefficient of rolling friction between LQ/MQ and aluminum | 0.052/0.052 |

### 3.2 Simulation repose angle

The coefficient of rolling friction of quinoa seeds was initially determined to be 0.01-0.11. The repose angle was scribed and linearly fitted with Excel and CAXA electronic drawing board software.

The calibration process is as follows: firstly, the simulation repose angle is colored in EDEM, and a screenshot is saved, then it is imported into CAXA electronic drawing board for scribing the contour, and a more uniform slope scribing is selected, finally, the data points were linearly regressed, and the repose angle was inversely derived from the slope of the linear equation. When the coefficient of rolling friction of LQ and MQ is 0.01, 0.03, 0.05, 0.07, 0.09, and 0.11, respectively, the repose angle formed in four directions are shown in Figure 11. The relationship between the repose angle and the coefficient of rolling friction are shown in Figure 12. The fitted linear are in Equations (7) and (8)

$$y = 99.612x + 22.668 \quad (7)$$

$$y = 120.79x + 25.687 \quad (8)$$

When the actual repose angle of LQ is 26.93°, the coefficient of rolling friction is 0.043 with Equation (7). When the actual repose angle of MQ is 27.68°, the coefficient of rolling friction is 0.016 with Equation (8). To verify the results reliability, the repose angle needs to be confirmed, as shown in Figures 13 and 14.

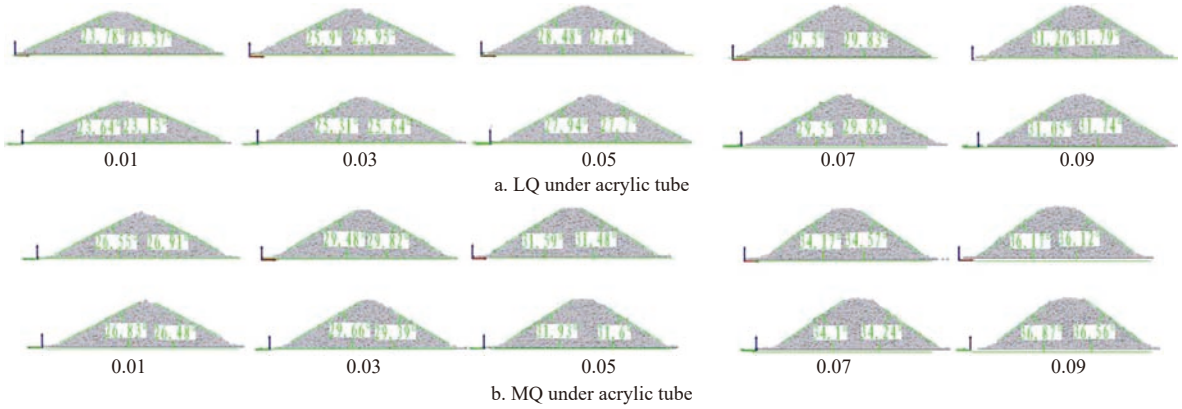


Figure 11 Simulation repose angle

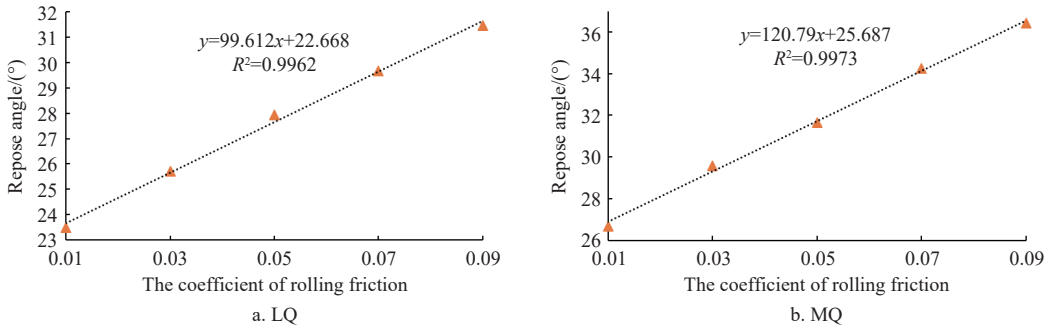


Figure 12 Relationship between the repose angle and coefficient of rolling friction

From Figure 13 and Figure 14, we can find that the simulation repose angle of LQ or MQ approach 26.9° or 27.7°, respectively. In addition, the simulation repose angle range of LQ or MQ is 70 mm or 65 mm. It shows that the quinoa seed model and the calibrated coefficient of rolling friction developed in this paper are reliable.

To reduce simulation time and improve efficiency, quinoa flat spherical seeds were modelled with a simplified 4-sphere model, which produces errors that are mainly compensated by calibrating their rolling friction coefficients, which have an important influence on the formation of the repose angle. To further investigate the effect of the coefficient of rolling friction on the formation of the repose angle, observations were made to study the changes in the trajectory lines of quinoa particles in the initial state at several different positions during the formation of the repose angle as influenced by the rolling friction coefficient.

### 3.3 Effect of coefficient of rolling friction on formation for repose angle

To investigate the influence of the coefficient of rolling friction on the seed in different positions of the cylinder during forming the repose angle, the seed models in 9 locations were manually selected, as shown in Figure 15a. The seed trajectories with vector mode were recorded, as shown in Figures 15b and 15c. Moreover,

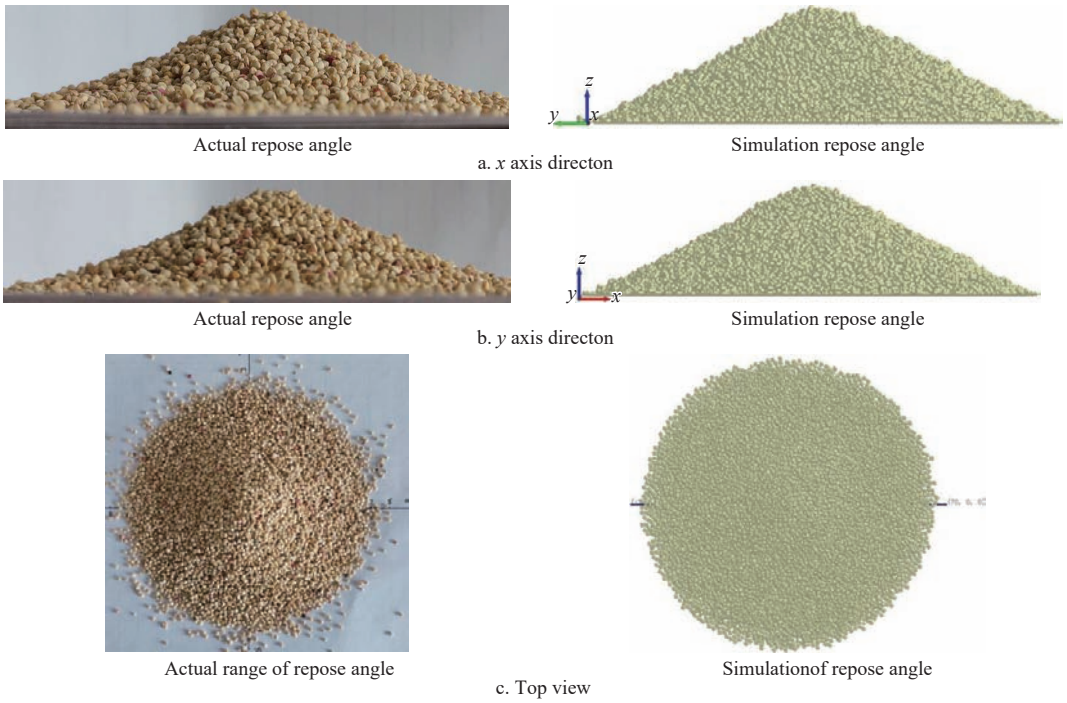


Figure 13 Verification results of the repose angle of LQ seeds

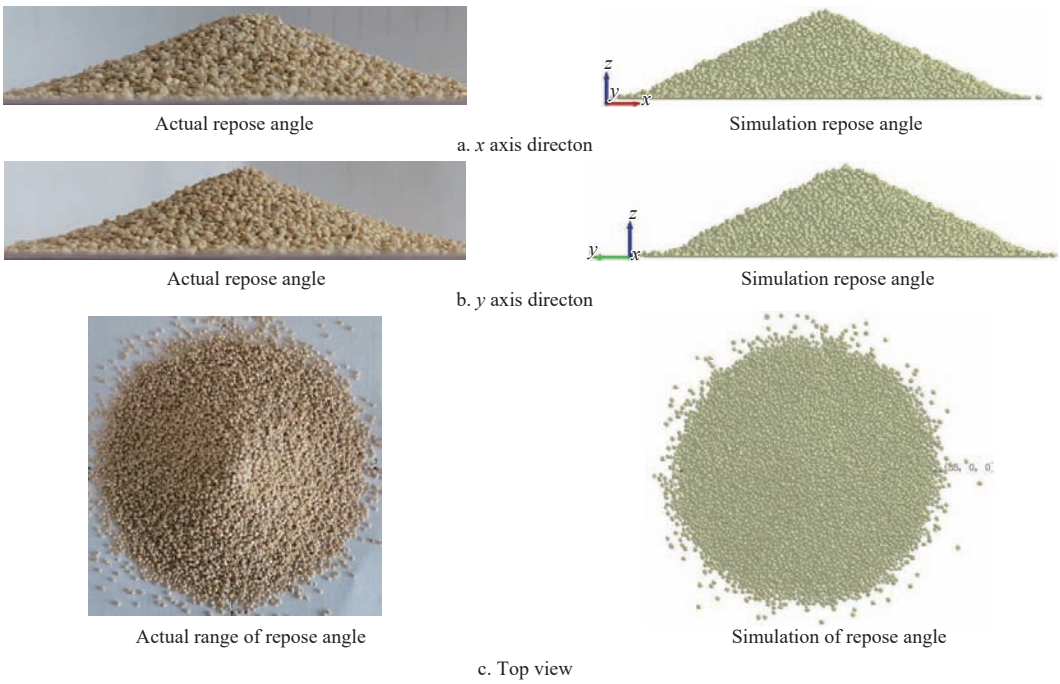


Figure 14 Verification results of the repose angle of MQ seeds

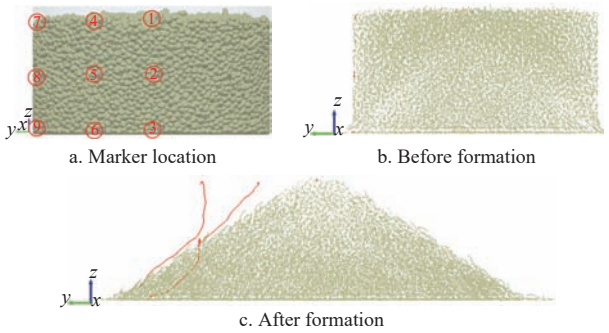


Figure 15 Formation of quinoa seed repose angle

the change of the seed positions, velocities, and angular velocities in the location 1, 4 and 7 with different coefficient of rolling friction are analyzed in detail, as shown in Figure 16.

By comparing Figures 15a and 15b, we found that the seed in location 4, 7, and 8 exhibit a pronounced descending trajectory, indicating that the seeds far from the center have a more significant energy change, which is converted into more incredible kinetic energy. Furthermore, to discover the seed trajectories change in the three locations of the first level, their angular velocity and the velocity were compared in detail, as displayed in Figure 16.

From Figure 16, changing the coefficient of rolling friction can not only change the seed angular velocity but also affect the velocity, which in location 7 significantly higher than those in position 4 and position 1. Although the seeds in the three locations are at a uniform height, the seeds in the middle position are better supported, and the gravitational potential energy is converted into

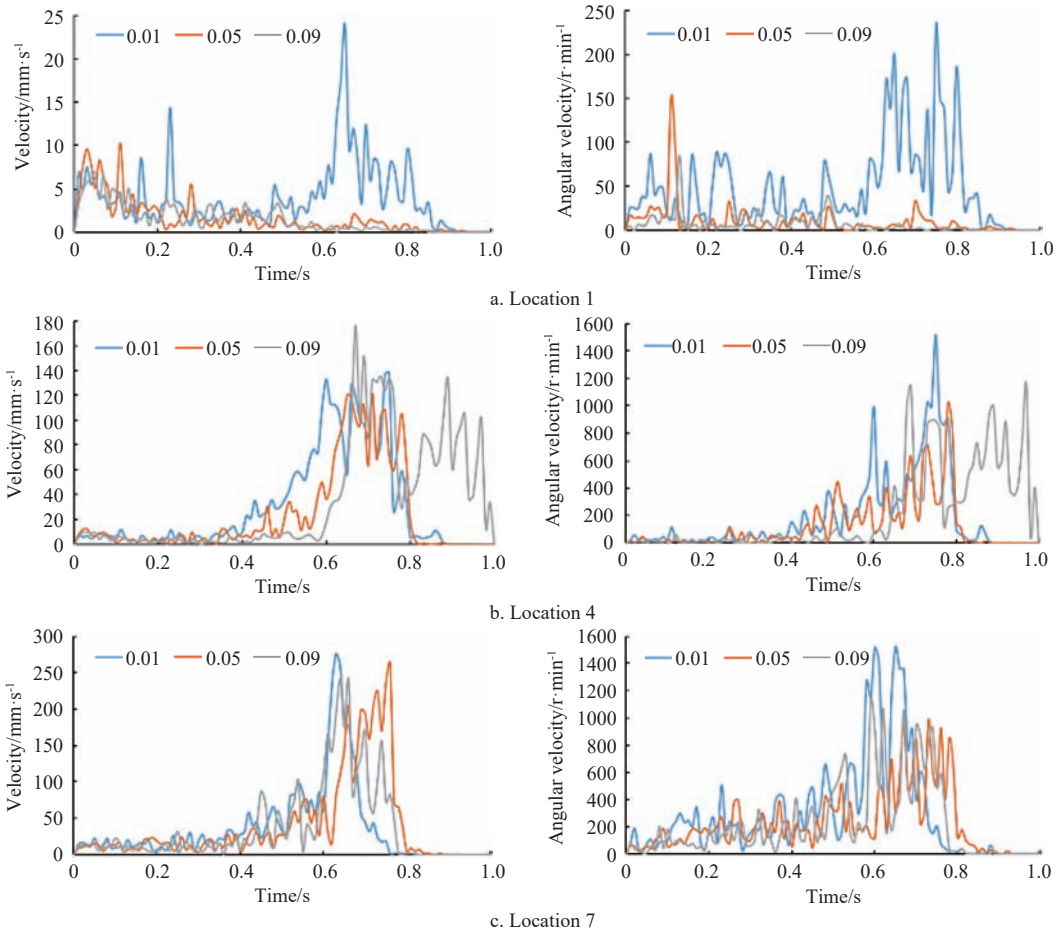


Figure 16 Velocity and angular velocity in forming repose angle

the kinetic energy of the efficiency is weaker, the seed in position 7 is not supported enough, gravitational potential energy is initially converted into downward translational kinetic energy, and in the process of falling is supported by the dynamic slope of the seed below, the potential energy and part of the translational kinetic energy is converted into rotational kinetic energy, and the rounded range of the repose angle ground is expanded.

## 4 Conclusions

(1) In this study, simulation parameters were determined and calibrated for two types of quinoa seeds, LQ and MQ. 3 direction dimensions, thousand-grain weight, mass density, bulk density, moisture content, Poisson's ratio, elastic modulus, shear modulus, coefficient of restitution, and the coefficient of static friction between quinoa seeds were mainly determined. The coefficient of rolling friction was calibrated on DEM, which of LQ is 0.043, and that of MQ is 0.016.

(2) The coefficient of rolling friction affects the seed velocity and angular velocity during forming repose angle. The seeds at different positions at the same height are affected by changing the coefficient of rolling friction. When the seeds falling, the seeds support force is the key to cause seeds rolling. The increasing coefficient of rolling friction of the seeds that are lack of support cannot affect their velocity and angular velocity. Meanwhile, the effect of the coefficient of rolling friction on non-spherical model is not always present. The shape can hinder and increase seeds rolling, while the coefficient of rolling friction strengthens the shape to restrict rolling and weakens the shape to increase rolling.

## Acknowledgements

This work was financially supported by China Agriculture Research System of MOF and MARA (Grant No. CARS-14-1-28), and. and Gansu Province Agricultural Science and Technology Innovation Project (Grant No. 2021GAAS23), and the National Natural Science Foundation of China grant number (Grant No. 52065004, 52365030).

## [References]

[1] Wiacek J, Molenda M, Horabik J, Ooi J Y. Influence of grain shape and intergranular friction on material behavior in uniaxial compression: Experimental and DEM modeling. Powder Technology, 2012; 217: 435–442.

[2] Coetzee C J. Review: Calibration of the Discrete Element Method. Powder Technology, 2017; 310: 104–142.

[3] Shi L R, Zhao W Y, Sun W, Yang X P, Wang G P, Xin S L. Analysis of the metering performance for typical shape maize seeds using DEM. Int J Agric & Biol Eng, 2023; 16(1): 26–35.

[4] Markauskas D, Kačianauskas R. Investigation of rice grain flow by multi-sphere particle model with rolling resistance. Granular Matter, 2011; 13: 143–148.

[5] Chen Z, Wassgren C, Veikle E, Ambrose K. Determination of material and interaction properties of maize and wheat kernels for DEM simulation. Biosystems Engineering. 2020; 195: 208–226.

[6] Shi L R, Sun W, Zhao W Y, Yang X P, Feng B. Determination of parameters and validation of discrete element simulation model for mechanical seeding of potato seed potatoes. Transactions of the CSAE, 2018; 34(6): 35–42.

[7] Guo J H, Zhao W Y, Shi L R, Zhou G, Zhang F W, Yang K S, Xin S L. Design and test of rolling spoon type flax combined seeder in the arid area of Northwest China, Journal of China Agricultural University, 2022; 27(7):

184–198.

[8] Boac J, Casada M E, Maghirang R, Harner J P. Material and interaction properties of selected grains and oilseeds for modeling discrete particles. Transactions of the ASABE, 53(4), 1201–1216.

[9] Shi L R, Zhao W Y, Yang X P. Effects of typical corn kernel shapes on the forming of repose angle by DEM simulation. Int J Agric & Biol Eng, 2022; 15(2): 248–255.

[10] Barrios G K P, de Carvalho R M, Kwade A, Tavares L M. Contact parameter estimation for DEM simulation of iron ore pellet handling. Powder Technology, 2013; 248: 84–93.

[11] Marigo M, Stitt E H. Discrete element method (DEM) for industrial applications: comments on calibration and validation for the modelling of cylindrical pellets. Kona Powder and Particle Journal, 2015; 32: 236–252.

[12] Vega-Gálvez A, Miranda M, Vergara J, Uribe E, Puente L, Martínez EA. Nutrition facts and functional potential of quinoa (Chenopodium quinoa willd. ), an ancient Andean grain: a review. J Sci Food Agric. 2010, 90(15): 2541–2547.

[13] Xiao Z C, Zhang G L. Quinoa and its resource development and utilization. Chinese Wild Plant Resources, 2014; 33(2): 62–66.

[14] Zhang Y F, Wu K M, Liu G Y, Ma S C. Effect of different harvesting periods on seed vigor and physical traits of wheat. Seed, 2021; 40(8): 1–7, 14.

[15] Sheng A L. A method for determining Young's modulus based on single slit diffraction. Physics Bulletin, 2014; 1: 77–78.

[16] Shi L R, Ma Z T, Zhao W Y, Yang X P, Sun B G, Zhang J P. Calibration of simulation parameters of flaxed seeds using discrete element method and verification of seed-metering test. Transactions of the CSAE, 2019; 35(20): 25–33.

[17] Yang Z, Li G F, Shi L R, Wang Z. Determination of the coefficient of static friction of maize seeds and validation of the discrete element method. Journal of Chinese Agricultural Mechanization, 2023; 44(8): 12–16.

[18] Gonzalez-Montellano C, Gallego E, Ramirez-Gomez A, Ayuga F. Three dimensional discrete element models for simulating the filling and emptying of silos: Analysis of numerical results. Computers & Chemical Engineering, 2012; 40: 22–32.

[19] Weigler F, Mellmann J. Investigation of grain mass flow in a mixed flow dryer. Particuology, 2014; 12: 33–39.

[20] Wang X M, Yu J Q, Lv F Y, Wang Y, Fu W. A multi-sphere based modeling method for maize grain assemblies. Advanced Powder Technology, 2017; 28(2): 584–595.

[21] Markauskas D, Kacianauskas R, Dziugys A, Navakas R. Investigation of the adequacy of multi-sphere approximation of elliptical particles for DEM simulations. Granular Matter, 2010; 12(1): 107–123.